JPET Fast Forward. Published on February 6, 2019 as DOI: 10.1124/jpet.118.256065
This article has not been copyedited and formatted. The final version may differ from this version.

JPET # 256065

Long-term engraftment of human cardiomyocytes combined with biodegradable microparticles induces heart repair

Laura Saludas*, Elisa Garbayo*, Manuel Mazo, Beatriz Pelacho, Gloria Abizanda, Olalla Iglesias-Garcia, Angel Raya, Felipe Prósper, María J. Blanco-Prieto

Department of Pharmaceutical Technology and Chemistry, School of Pharmacy and Nutrition, University of Navarra, Pamplona, Spain (L.S., E.G., M.B.P.)

Instituto de Investigación Sanitaria de Navarra (IdiSNA), Pamplona, Spain (L.S., E.G., M.M., B.P., G.A., F.P., M.B.P.)

Hematology and Cell Therapy, Clínica Universidad de Navarra and Foundation for Applied Medical Research, Pamplona, Spain (M.M., B.P., G.A., F.P.)

Center of Regenerative Medicine in Barcelona, Barcelona, Spain (O.I., A.R.)

* Both authors contributed equally to this work

This work was supported by the Spanish Ministry of Economy and Competitiveness [SAF2013-42528-R, SAF2017-83734-R and Cardiomesh], funds from the ISCIII and FEDER [Tercel RD16/0011/0005, PI16/00129, CPII15/00017 and ERANET II-Nanoreheart], "Asociación de Amigos de la Universidad de Navarra" and "la Caixa" Banking Foundation.

Running Title: hiPSC-CMs-laden MPs repair the heart after a MI

Corresponding author:

Maria J. Blanco-Prieto, PhD

Department of Pharmaceutical Technology and Chemistry, School of Pharmacy and Nutrition, University of Navarra, C/ Irunlarrea 1, 31008 Pamplona, Spain.

Tel: +34 948 425 600 ext. 806519 Fax: +34 948 425 619

E-mail: mjblanco@unav.es

Number of text pages: 37

Number of tables: 1

Number of figures: 5

Number of references: 44

Number of words in the abstract: 240

Number of words in the introduction: 742

Number of words in the discussion: 1418

Nonstandard abbreviations: CMs, cardiomyocytes; EDV, end-diastolic volume; ESV, end-systolic volume; FAC: fractional area change; FACS: fluorescence-activated cell sorting; hiPSC, human induced pluripotent stem cells; hiPSC-CMs, cardiomyocytes-derived from human induced pluripotent stem cells; HSA, human serum albumin; LVEF: left ventricle ejection fraction; MI, myocardial infarction; MPs, microparticles; PBS, phosphate buffered saline; PDL, poly-D-lysine; PEG, polyethylene glycol; PLGA, poly(lactic-co-glycolic) acid; PVA, poly(vynil alcohol).

Recommended section assignment: Special Section Articles

Abstract

Cardiomyocytes derived from human induced pluripotent stem cells (hiPSC-CMs) are a promising cell source for cardiac repair after myocardial infarction (MI) as they offer several advantages, such as potential to remuscularize infarcted tissue, integration in the host myocardium and paracrine therapeutic effects. However, cell delivery issues have limited their potential application in clinical practice, showing poor survival and engraftment after transplantation. In this work, we hypothesized that the combination of hiPSC-CMs with microparticles (MPs) could enhance the long-term cell survival and retention in the heart and consequently improve cardiac repair. CMs were obtained by differentiation of hiPSC by small-molecule manipulation of the Wnt-pathway, and adhered to biomimetic poly(lactic-co-glycolic acid) MPs covered with collagen and poly-D-lysine. The potential of the system to support cell survival was analyzed *in vitro*, demonstrating a 1.70-fold and 1.99-fold increase in cell survival after 1 and 4 days, respectively. The efficacy of the system was tested in a mouse MI model. Interestingly, two months after administration, transplanted hiPSC-CMs could be detected in the peri-infarct area. These cells not only maintained the cardiac phenotype but also showed *in vivo* maturation and signs of electrical coupling. Importantly, cardiac function was significantly improved, which could be attributed to a paracrine effect of cells. These findings suggest that MPs represent an excellent platform for cell delivery in the field of cardiac repair, which could also be translated into an enhancement of the potential of cell-based therapies in other medical applications.

Introduction

Myocardial infarction (MI) continues to represent the leading cause of mortality and morbidity worldwide (Reed *et al.*, 2017). Despite the great medical advances in recent years, treatments are still palliative, with heart transplant constituting the only option providing a definite and reparative solution. However, it is severely limited by the availability of donors and major complications associated with such an invasive procedure (Tonsho *et al.*, 2014). After a MI, it is estimated that 50 g of the human heart muscle becomes dysfunctional due to the irreversible loss of around 1 billion native cardiac cells (Gepstein, 2002). The endogenous regenerative mechanisms of the heart are insufficient to replace the dead tissue, which remains chronically impaired. Therefore, a large number of patients that suffer from a cardiac ischemic event undergo frequent rehospitalizations, multimedication and progress towards end-stage heart failure (Bahit *et al.*, 2018).

Cardiac cell therapy arose at the turn of the century as a novel strategy aiming to counteract the massive loss of tissue by repopulating the ischemic area with functional cardiac lineage cells. Since then, a large number of cell sources have been explored in preclinical studies with several progressing to the clinical stage (Telukuntla *et al.*, 2013). As cardiomyocytes (CMs) are responsible for heart contraction, many efforts have been focused on the development of *in vitro* protocols to generate contractile cardiac muscle cells similar to native heart cells (Boheler *et al.*, 2002; Batalov and Feinberg, 2015). So far, embryonic stem cells have been the major source for obtaining CMs (Liu *et al.*, 2018). However, ethical, immunogenic and availability issues have limited their potential application (Nussbaum *et al.*, 2007). Recently, the generation of induced pluripotent stem cells (iPSC) from adult cells by Yamanaka et al. (Takahashi and Yamanaka, 2006) and the progresses in cell reprogramming techniques came to provide another attractive source of CMs. CMs differentiated from iPSC (iPSC-CMs) present potential advantages. These cells can be expanded to obtain a large number of cells, are non-immunogenic (autologous) and do not require the destruction of embryonic tissue (Lalit *et al.*, 2014; Cahill *et al.*, 2017).

Research conducted over the last few years on cell therapy has taught us several lessons. Originally, it was believed that transplanted stem cells develop into cardiac cell types. However, when the fate of engrafted cells was investigated, most of the studies reported that only a few cells, if any, actually gave rise to new cells (Nigro *et al.*, 2018). Instead, cells were found to stimulate cardiac functional recovery by the secretion of a wide variety of biologically active molecules that modulate nearby cells behaviour, which is known as the paracrine effect (Hodgkinson *et al.*, 2016). Moreover, efficacy results originated from these studies have been controversial due to the low percentage of local engraftment and survival of transplanted cells (Hou *et al.*, 2005; Terrovitis *et al.*, 2010).

In this framework, the association of stem cells and drug delivery systems is now taking cell therapy one step further. Biocompatible implantable/injectable hydrogels have been extensively explored to deliver and retain cells in the target tissue, bringing significant improvements in cardiac function (Saludas *et al.*, 2017). However, these systems have also shown limitations, such as lack of long-term cell engraftment (Chow *et al.*, 2017), administration procedures based on open-chest surgeries (Atluri *et al.*, 2014) or need for a careful adjustment of the gelation and mechanical properties. An alternative less widely investigated approach to deliver cells could be the use of biodegradable and biocompatible microparticles (MPs) (Saludas *et al.*, 2018). MPs represent an excellent delivery platform, as they allow for minimally invasive administration procedures using catheter technology (Garbayo *et al.*, 2016) and are localizable to the injection site (Leong and Wang, 2015). Among the diverse cell-based applications, MPs may be used as tridimensional scaffolds, as microcapsules or as key elements to deliver molecules and control the architecture of cell aggregates (Ahrens *et al.*, 2017).

In this study, we developed an effective strategy for cardiac repair by the combination of human iPSC-CMs (hiPSC-CMs) and biomimetic MPs. First, cell-MP complexes were prepared and *in vitro* cell viability was analyzed. We then studied the potential of the strategy to enhance long-term hiPSC-CMs survival and engraftment in a mouse MI model, and its impact on cardiac function and adverse ventricular remodeling. Finally, the phenotype, electrical coupling and

maturation of the engrafted cells were characterized. Altogether, the results obtained indicate that the combination of hiPSC-CMs with MPs is a promising approach to stimulate heart repair after a MI.

Materials and Methods

Materials

Poly(lactic-co-glycolic acid) (PLGA) with a monomer ratio (lactic acid/glycolic acid) of 50:50 Resomer® RG 503H (Mw: 34 kDa) was provided by Boehringer-Ingelheim (Ingelheim, Germany). Polyethylene glycol (PEG, Mw: 400 Da), human serum albumin (HSA), Sigmacote®, fibronectin from bovine plasma, poly-D-lysine (PDL), cadmium chloride, Fast Red, hydrochloric acid, rabbit anti-connexin-43 antibody (C6219) and rabbit anti-α-sarcomeric actinin (A7811) were provided by Sigma-Aldrich (Barcelona, Spain). Dichloromethane, acetone and formaldehyde were obtained from Panreac Química S.A. (Barcelona, Spain). Poly(vinyl alcohol) (PVA) 88% hydrolyzed (Mw: 125 kDa) was obtained from Polysciences, Inc. (Warrington, PA, USA). Collagen I rat protein and phosphate buffered saline pH 7.2 (PBS) were provided by Gibco-Invitrogen (Carlsbad, CA, USA). Live/Dead™ Viability/Cytotoxicity kit was obtained from Molecular Probes (Carlsbad, CA, USA). Mouse anti-human mitochondria (ab92824) and rabbit anti-dystrophin (ab15277) primary antibodies were purchased from Abcam (Cambrigde, UK). Alexa Fluor 488 goat anti-mouse (A10680) and Alexa Fluor 594 goat anti-rabbit (A11012) secondary antibodies were supplied by Invitrogen (Carlsbad, CA, USA). Anti-cardiac troponin T (MA5-12960), AlamarBlue™ Cell Viability Reagent, the Human Episomal iPSC Line, Essential 8™ Medium, RPMI basal medium, B27 and B27 minus insulin supplements, as well as other cell culture reagents were obtained from ThermoFisher (Carlsbad, CA, USA). Small molecules CHIR99021 and C-59 were from Axon Medchem (Groningen, The Netherlands), while ROCK inhibitor Y27632 was purchased from Tocris (Bristol, UK) and Growth Factor Reduced Matrigel Matrix from BD Bioscience (Madrid, Spain).

Differentiation and isolation of CMs from hiPSCs

CMs were obtained by differentiation of hiPSCs as described in (Lian *et al.*, 2013). Briefly, cells were maintained in Essential 8 Medium on 1:180 Growth Factor Reduced Matrigel coated plates

until subconfluence, when hiPSCs were routinely passaged at a 1:15 ratio. For differentiation, cells were plated on 12-well plates as above. When the culture reached 80-90% confluence, the medium was changed to RPMI supplemented with 1X B27 minus insulin (RPMI-minus insulin) plus 8 μM CHIR99021 for 24 hours. Then, the medium was replaced with RPMI-minus insulin for 48 hours, followed by 5 μM C-59 in RPMI-minus insulin for another 48 hours. Next, the medium was shifted again to RPMI-minus insulin for 48 hours, before changing to RPMI supplemented with 1X B27 (RPMI-B27). This medium was renewed every other day until the appearance of beating (usually 7-9 days after the start of the differentiation), when a metabolic selection of hiPSC-CMs by culturing for 72 hours in RPMI without glucose supplemented with 1X B27 and 4 mM Lactate was applied. Cells were returned to conventional RPMI-B27 for 48 hours before another 72 hours of metabolic selection in the above mentioned medium. After that, cells were returned to RPMI-B27 for 48 hours and isolated. At this point hiPSC-CMs formed beating monolayers. For this, cells were washed 3 times with PBS plus 0.5 mM EDTA, and incubated for 7-15 minutes in warm TryplE. hiPSC-CMs were then mechanically dissociated with a micropipette tip and counted with trypan blue to exclude dead cells. The required amount of cells was suspended in RPMI-B27 plus 1 μM Y27632 and spun down at 1000 rpm for 10 minutes.

Characterization of hiPSC-CMs

Differentiation purity was assessed by fluorescence-activated cell sorting (FACS), while hiPSC-CMs identity was confirmed by functionality (beating), gene and protein expression. For FACS, cells were stained with anti-cardiac Troponin T (1:100, MA5-12960) using the Fix & Perm kit and analyzed. RNA extraction was carried out with TRIreagent®, while RT was performed using TaKaRa PrimeScript RT Reagent Kit, following the manufacturer´s instructions, with a maximum of 500 ng of RNA per sample. RT-qPCR was performed with primers shown in Supplemental Table 1, using Applied Biosystems™ PowerUp™ SYBR™ Green Master Mix in a QuantStudio 5 (Thermo Fisher Scientific). GAPDH was selected as a housekeeping gene and the results were

analyzed using the $2^{-\Delta\Delta Ct}$ method. For protein expression, cells were labelled with anti-α-sarcomeric actinin (1:200, A7811) and visualized with a Zeiss confocal microscope.

Preparation of MPs

PLGA particles were prepared by the multiple emulsion solvent evaporation method using Total Recirculation One-Machine System (TROMS) (Formiga *et al.*, 2013; Pascual-Gil *et al.*, 2015). Briefly, the organic phase (O) consisting in 50 mg of PLGA 503H dissolved in a mixture of 4 ml of acetone/dichloromethane (1:3) was injected into the inner aqueous phase (W_1) formed by 5 mg of HSA, 5 µl of PEG 400 and 200 µl of PBS pH 7.4. The W_1/O emulsion was allowed to recirculate through the system for 1 min and 30 sec. Then, this emulsion was added to the outer aqueous phase (W_2) consisting of 20 ml of PVA 0.5% and allowed to recirculate for 2 mins and 30 sec. Finally, the $W_1/O/W_2$ emulsion was stirred at RT for 3 hours to allow total solvent evaporation. MPs were washed three times with ultrapure water by consecutive centrifugation at 20,000 G, 4ºC for 5 mins and lyophylized for 48 hours (VirTis Genesis Freeze Dryer 12 EL, Gardiner, New York, USA). Lyophilized MPs were stored at 4ºC.

Characterization of MPs

Particle size, size distribution and zeta potential were determined after lyophilization. Particle size and size distribution were measured by laser diffractometry using a Mastersizer® (Malvern Instruments, Malvern, UK). MPs were dispersed in ultrapure water and analyzed under continuous stirring. The average particle size was expressed as the volume mean diameter. Particle surface charge was determined by zeta potential measurement using a Zetasizer Nano ZS (Malvern Instruments, Malvern, UK), based on the analysis of complete electrophoretic mobility distributions.

Particle surface modification

In order to facilitate the adhesion of hiPSC-CMs to MPs, particle surface was functionalized by coating with biomimetic molecules. Different mixtures of molecules and concentrations were tested to select the most adequate to favor the adhesion of hiPSC-CMs. The different coatings studied were: I) a mixture of 30 µg/ml of collagen type I and 100 µg/ml of PDL, II) a mixture of 60 µg/ml of collagen type I and 100 µg/ml of PDL and III) a mixture of 30 µg/ml of fibronectin and 100 µg/ml of PDL. In all cases, particle coating was performed in sigmacoted tubes. MPs were dispersed in acidified PBS (pH 5.7). Then, biomimetic molecules were added to the particles solution and the mixtures were incubated at 37ºC for 1 hour under rotation. Coated particles were washed with distilled sterile water by consecutive centrifugations (25,000 G, 4ºC, 10 mins) and lyophilized for 48 hours. Zeta potential was measured to confirm that the particles had been successfully coated.

Adhesion of hiPSC-CMs to MPs

For the adhesion of cells, 0.150 mg of coated MPs were dispersed in RPMI-B27 medium prior to the addition of 150,000 CMs. The mixture was plated in a Costar® Ultra Low Cluster Flat Bottom Sterile Polystyrene Plate and incubated at 37ºC. The evolution of the adhesion of cells to MPs was assessed at 30 mins, 1, 1.5, 2 and 4 hours by bright field microscopy (Nikon TMS, Amsterdam, Netherlands).

***In vitro* cell survival**

The survival of cells cultured alone or adhered to MPs was evaluated by Live/Dead® and Alamar Blue assays, following manufacturer's instructions. For that, 150,000 cells alone or 150,000 cells adhered to 0.150 mg of MPs were incubated in Costar® Ultra Low Cluster Flat Bottom Sterile Polystyrene Plate at 37ºC. After 1 day and 4 days of incubation, samples were stained with

Live/Dead staining kit for 30 min at 37ºC, and then examined using a LSM 800 confocal microscope (Zeiss, Madrid, Spain). The survival rate of cells was quantified by incubation with Alamar Blue kit at 37ºC. After 6h of incubation, absorbance was measured at 570 nm and 600 nm using a Power Wave XS Microplate Spectrophotometer. Survival was calculated following manufacturer's instructions. Four to eight replicates were used in each treatment and the test was performed in quadruplicate.

In vivo studies using chronic MI model

All animal procedures were approved by the Institutional Animal Care and Use Committee of the University of Navarra and performed according to the requirements of the EU legislation.

Permanent myocardial ischemia was induced in male BALB/C (Rag-2) mice aged 8-12 weeks. Briefly, animals were anesthetized with isoflurane and intubated for mechanical ventilation. Prior to surgery, animals received ketoprofen, fentanest and enrofloxacin. Mice underwent a left thoracotomy through the fourth intercostal space and the left anterior descending coronary artery was permanently occluded. After 15 min of artery occlusion, the animals received one of these treatments: MPs coated with PDL and collagen (0.150 mg, n=13) or hiPSC-CM-MPs (150,000 hiPSC-CMs adhered to 0.150 mg of MPs coated with PDL and collagen, n=11). Treatments were dispersed in 12 µl of injection medium and injected intramyocardially into two areas using a 27G syringe. Finally, animals were closed, administered with buprex and allowed to recover.

Cardiac function evaluation

Echocardiography was performed using a Vevo 770 ultrasound system (Visualsonics, Toronto, Canada) at 2 and 60 days following ligation of the left anterior descending coronary artery. Measurements were optimized for small animals and performed as previously described (Benavides-Vallve *et al.*, 2012). Left ventricle ejection fraction (LVEF), fractional area change

(FAC), end-systolic volume (ESV) and end-diastolic volume (EDV) were studied. A total of 24 animals with a LVEF below 45% at day 2 post-MI were included in the study.

Morphometric and histological studies

Male mice were sacrificed at day 7 (n=4 for MPs group, n=3 for hiPSC-CM-MPs group) or at day 60 (n=9 for MPs group, n=8 for hiPSC-CM-MPs group) to perform the morphometric and histological studies. Briefly, mice were anesthetized, injected with 100 µl of 0.1 mM cadmium chloride for diastole cardiac arrest, and perfusion-fixed for 15 min with Zn-Formalin under physiological pressure. The hearts were excised, fixed o/n in Zn-Formalin at 4ºC, cut into 3 equally-sized blocks (apical, mid-ventricular, and basal), dehydrated in 70% ethanol (4°C, o/n), and embedded in paraffin. For histological analysis, 5 µm serial sections were prepared.

Infarct size and heart wall thickness were determined using Sirius Red stained sections. For the Sirius Red staining, sections were deparaffinized and immersed for 90 min in 0.1% Fast Red, which was diluted in a saturated solution of picric acid. They were then differentiated for 2 min in 0.01 N HCl, dehydrated and mounted in DPX. Infarct size was assessed by quantifying images from 12 serial heart sections, 50 µm apart. Images were analyzed with Image J 1.48v software and data were expressed as a percentage of the ischemic area *vs.* the total left ventricle area. For quantifying infarct wall thickness, 12 images from serial heart sections of the infarct zone were analyzed using Image J 1.48v software.

The survival and engraftment of transplanted cells was analyzed and quantified at 7 days and 60 days post-administration in the ischemic tissue. Due to the human origin of transplanted cells, these cells could be identified *in vivo* by immunostaining using a mouse anti-human mitochondria antibody (1:1000, ab92824). The number of engrafted cells was calculated by quantifying images from 15 serial heart sections 50 µm apart, and extrapolating this number to the whole length of the graft area. Data were expressed as a percentage of the number of engrafted cells vs. the number of injected cells. Electrical coupling of transplanted cells and preservation of the cardiac

phenotype were studied using rabbit anti-connexin-43 (1:500, C6219) and rabbit anti-dystrophin antibodies (1:100, ab15277), respectively. In addition, Alexa Fluor 488 goat anti-mouse (1:200, A10680) and Alexa Fluor 594 goat anti-rabbit (1:200, A11012) secondary antibodies were used. Fluorescently stained tissue slides were observed with a camera attached to a Zeiss Axio Imager M1 fluorescence microscope.

Statistical analysis

Statistical analysis was performed using GraphPad Prism 5.0 (Graphpad Software Inc., San Diego, CA, USA). Differences between both groups for each time point were analyzed by a t test for independent samples. Results are expressed as mean ± SEM. Statistical significance was determined by p values < 0.05.

Results

Cardiac differentiation of hiPSCs

Cardiac differentiation was performed by small-molecule manipulation of the Wnt-pathway, followed by enrichment through metabolic selection (Fig. 1A). This resulted in the final obtaining of beating monolayers of hiPSC-CMs (Supplementary Video 1), with all experiments showing a purity above 90% of cardiac Troponin T-positive cells by FACS (Fig. 1B). RT-qPCR analysis (Fig. 1C) showed a robust downregulation of pluripotency-associated genes (NANOG, PU5F1 and SOX2), concomitant with an upregulation of a cardiac-specific gene expression profile (NKX2-5, GATA4, MEF2C, MYH6, MYH7, MYL2, MYL7 and HCN4). hiPSC-CMs were mononucleated, with well-defined sarcomeres, as depicted by α-sarcomeric actinin staining (Fig. 1Di, ii).

Microparticle characterization

MPs were manufactured using PLGA, a biocompatible and biodegradable FDA-approved polymer as a model system (Makadia and Siegel, 2011). PLGA MPs were prepared by the multiple emulsion solvent evaporation method using TROMS. A homogenous population of MPs with a mean particle size of 10.4 ± 0.8 μm was obtained. Particles presented a negative surface charge with a zeta potential of -20.4 ± 3.3 mV.

Particle surface modification

The surface of particles was functionalized with biomimetic molecules to facilitate the adhesion of hiPSC-CMs. Collagen type I and fibronectin are proteins of the cardiac extracellular matrix that bind cell adhesion molecules on the surface of cells, while PDL increases the surface charge of MPs to positive values. This switch of zeta potential may attract cells by non-specific interactions between the negatively charged cell membrane and the positively charged surface of

MPs (Delcroix *et al.*, 2011; Garbayo *et al.*, 2011). Zeta potential was measured to confirm the successful coating. All coated particles presented positive zeta potential values, with those particles coated with a larger proportion of PDL presenting higher values. In particular, the coating of MPs with 30 µg/ml of collagen and 100 µg/ml of PDL increased zeta potential to +20.0 ± 2.2 mV, the coating with 60 µg/ml of collagen and 100 µg/ml of PDL to +16.3 mV and the coating with 30 µg/ml of fibronectin and 100 µg/ml of PDL to +25.0 mV.

Adhesion of hiPSC-CMs to MPs

The evolution of the adhesion of hiPSC-CMs to MPs with different coatings was studied at 30 mins, 1, 1.5, 2 and 4 hours by bright field microscopy. On the one hand, when cells were incubated with MPs covered with 30 µg/ml of fibronectin and 100 µg/ml of PDL, only a small number of cells were adhered to particles after 1.5 hours of incubation (Fig. 2A). By contrast, the coating of particles with 30 or 60 µg/ml of collagen and 100 µg/ml of PDL induced a greater adhesion of hiPSC-CMs. After 1.5 hours of incubation, most of the cells were successfully adhered to the surface of particles (Fig. 2A). Incubation for longer times did not increase cell adhesion. Similar results were obtained in terms of particle surface charge and cell adhesion properties with both concentrations tested of collagen, which suggests that 30 µg/ml of collagen creates a large enough biomimetic surface for the adhesion of 150,000 hiPSC-CMs. From a practical point of view, the coating formed by the lowest concentration of collagen blended with PDL (i.e. 30 µg/ml of collagen and 100 µg/ml of PDL) was selected for further studies to obtain a less expensive protocol with potential for future clinical translation.

***In vitro* survival of cells**

The potential of MPs to provide cells with a 3-dimensional microenvironment that enhances cell survival and facilitates cell biological functions was analyzed by the Live/Dead and Alamar Blue assays. As seen in the Live/Dead assay, after 1 day of incubation the number of viable cells was

increased when cells were cultured associated with MPs compared to cells alone (Fig. 2B). This higher survival was maintained up to day 4. These results were quantified and confirmed with the Alamar Blue assay. The use of particles as a physical support for cells produced a significant 1.7-fold increase in cell survival over the culture of cells alone after 1 day and a 1.99-fold increase after 4 days. These results demonstrate that the adhesion of cells to the surface of biomimetic MPs stimulates cell viability by providing cells with a 3-dimensional support.

Cardiac functional analysis

We then tested the efficacy of the complexes to repair the damaged myocardium in a mouse MI model. LVEF, FAC, ESV and EDV were analyzed by echocardiography at 2 and 60 days post-treatment administration. After 2 days, no differences could be found between MPs and hiPSC-CM-MPs groups for any of the functional parameters studied. Two months after treatment administration, LVEF was significantly enhanced ($p < 0.05$) in animals treated with hiPSC-CM-MPs (41.25 ± 2.57 %) compared to animals treated with MPs (33.21 ± 1.86 %) (Fig. 3A). Similar results were obtained when FAC was studied. This parameter was significantly increased ($p < 0.05$) in the hiPSC-CM-MPs group (30.31 ± 2.28 %) compared to the MPs group (23.26 ± 1.46 %) (Fig. 3B). Furthermore, functional analysis revealed that pathological hypertrophy of the left ventricle was prevented after 2 months in the combinatorial treatment, as reflected in the ESV and EDV parameters. In this sense, a significant reduction was found in the hiPSC-CM-MPs group compared to the MPs group in both ESV (MPs: 96.95 ± 8.21 µl, hiPSC-CM-MPs: 63.16 ± 3.09 µl, $p < 0.01$) and EDV (MPs: 142.70 ± 8.77 µl, hiPSC-CM-MPs: 111.80 ± 4.8 µl, $p < 0.05$) (Fig. 3C and D). These findings reveal that the combinatorial use of hiPSC-CMs and MPs as a therapeutic option is able to induce significant cardiac repair, as shown by the improvement in cardiac function.

Morphometric and histological studies

Left ventricle remodeling

Left ventricle wall thickness and infarct size were analyzed after 2 months of treatment administration. Left ventricle wall thickness was slightly increased in the animals treated with hiPSC-CM-MPs (499.0 ± 41.7 μm) compared to animals treated only with MPs (446.2 ± 58.4 μm) (Fig. 4A). Similarly, a tendency towards a reduction of infarct size was observed in the hiPSC-CM-MPs group (19.93 ± 2.91 %) compared to MPs group (25.09 ± 4.28 %) (Fig. 4B). These findings may suggest that MPs alone or in combination with cells induce a similar prevention of adverse ventricle remodeling.

Fate of transplanted cells

The engraftment and survival of transplanted hiPSC-CMs was analyzed at one week and two months post-administration in the ischemic tissue by immunofluorescence using an anti-human mitochondria antibody, that allows the specific detection of cells of human origin. One week after administration, transplanted cells could be detected at the graft site in the infarct and peri-infarct area. hiPSC-CMs were relatively small, presented a round-shape morphology and were arbitrarily distributed. Interestingly, when cell survival was analyzed after 2 months, engrafted cells could still be detected at the injection site surrounding the damaged area (<1%) (Fig. 5A). At this time, engrafted cells showed a certain maturation reflected in their larger and elongated morphology and the appearance of clusters of aligned hiPSC-CMs. Additionally, engrafted cells preserved their cardiac phenotype as reflected in the expression of dystrophin throughout the cytoplasm (Fig. 5B). Finally, we investigated whether engrafted cells formed gap junctions with other cells and therefore, if they showed signs of electrical coupling to native cardiac cells. For that, the expression of Cx-43 was analyzed. After 2 months of administration in the cardiac tissue, transplanted hiPSC-CMs showed expression of Cx-43 at the interface between transplanted hiPSC-CMs (Fig. 5C). Altogether, the results indicate that the transplantation of cells in combination with MPs enhances cell survival and engraftment. In addition, engrafted hiPSC-CMs

maintain a cardiac muscle phenotype and express cardiac Cx-43 gap-junction protein after 2 months of administration.

Discussion

In this paper, we have effectively developed a strategy for cardiac repair based on the enhancement of hiPSC-CM therapy potential through combination with biomimetic MPs. Given that the low survival of cells in the cardiac tissue critically limits the clinical application of cell therapy, the main goal of this study was to implement a system to improve long-term cell engraftment. Specifically, *in vitro* studies revealed that the combination of hiPSC with biomimetic MPs enhanced cell survival compared to cells alone, indicating the potential of MPs to support cell functions. In consonance, the transplantation of hiPSC-CMs associated with biomimetic MPs in a mouse MI model notably increased cell survival up to 2 months. After this period, engrafted cells showed maturation and expression of Cx-43 gap-junction protein. Importantly, progress in cell delivery shown in this study correlated with a cardiac functional improvement, mainly attributed to a paracrine effect of cells. Overall, these results highlight the potential of MPs to overcome cell delivery issues, which could be translated into a greater stimulation of heart repair.

Numerous preclinical and clinical studies have been conducted aiming to elucidate the cell source that presents the largest potential to stimulate the repair of the necrotic myocardium (Yu *et al.*, 2017). In a previous study, our group demonstrated that the transplantation of adipose-derived stem cells combined with MPs enhances cardiac repair in a rat MI model (Díaz-Herráez *et al.*, 2017). However, when the fate of transplanted cells was analyzed, adipose-derived stem cells did not differentiate to CMs. Lack of stem cell differentiation is similarly a constant in other studies (Lin *et al.*, 2010). Transplantation of differentiated CMs could bring some advantages. Injection of cells similar to the native myocardium is related to the mechanical and functional coupling of cells, which reduces the appearance of arrhythmias (Pijnappels et al., 2010). Additionally, Tachibana et al. recently described that hiPSC-CMs salvage the myocardium more effectively than hiPSC through their differential paracrine secretion (Tachibana *et al.*, 2017). Nowadays, the only realistic CM source are hiPSCs. Furthermore, as it has been demonstrated in this paper and by other authors, it is possible to apply robust differentiation protocols to generate CMs that can be implemented in regenerative therapies (Wang *et al.*, 2016; Breckwoldt *et al.*, 2017).

One of the most interesting findings in the present study is the demonstration that MPs are powerful carriers to improve cell survival both *in vitro* and *in vivo*. Previous studies showed that the number of cells remaining in the cardiac tissue after a few hours is extremely low (Hou *et al.*, 2005; Terrovitis *et al.*, 2010). Interestingly, in a previous study where hiPSC-CMs were injected in a mouse MI model, 3.8% cells could be found at 7 days, 0.3% at 14 days and no cells were found at 1 and 2 months after administration (Iglesias-García *et al.*, 2015). In this paper, we were able to localize engrafted cells in the cardiac tissue after 2 months, which hugely encourage the potential of particles to support cell viability. The positive impact that the association with particles has on cell viability and engraftment can be explained by different mechanisms. Although traditionally used for protein encapsulation (Pascual-Gil *et al.*, 2015; Garbayo *et al.*, 2016; Suarez *et al.*, 2016) rather than cell delivery, MPs also constitute suitable scaffolds to provide cells with a biomimetic tridimensional support (Díaz-Herráez *et al.*, 2013). Furthermore, our group proved that MPs similar to those employed in this paper are retained in the myocardium for up to three months, avoiding mechanical washout of cells from the heart (Formiga *et al.*, 2013). With the same aim of overcoming the low engraftment of cells, other authors have explored the delivery of hiPSC-CMs encapsulated in hydrogels (Wang *et al.*, 2015; Chow *et al.*, 2017). Wang et al. found an increased survival of hiPSC-CMs in the heart after transplantation in the hydrogel matrix at 2 weeks, but survival rates were not studied at longer times (Wang *et al.*, 2015). On the other hand, despite the encouraging results in terms of cardiac repair, Chow et al. reported the absence of grafted cells after 10 weeks when transplanted in a synthetic PEG hydrogel (Chow *et al.*, 2017), a similar end-point to ours. In view of these results, we suggest that biomimetic MPs could constitute better cell delivery platforms than hydrogels. Further studies using natural hydrogels and hiPSC-CMs would help to compare results with both delivery systems.

Going a step further, our data demonstrates that hiPSC-CM grafts showed a certain degree of maturation in the cardiac tissue, with a larger size and elongated morphology after 2 months. In addition, clusters of cells could be found in an aligned disposition, which could reveal integration within the surrounding myocardium. We have also shown that cells expressed dystrophin after 2

months, which confirms that engrafted cells maintained their cardiac phenotype. In the literature there are only a few studies describing the *in vivo* engraftment, maturation and alignment of transplanted cells in the infarcted myocardium in the long term. One example is the work recently carried out by Liu et al. (Liu *et al.*, 2018), where authors found a similar *in vivo* maturation of CMs derived from embryonic stem cells. Integration in the native myocardium could be suggested by the expression of the gap junction protein Cx-43 observed in grafted cells. Expression of this protein could be related to the electrical coupling of cells and protection against ventricular arrhythmias (Roell *et al.*, 2007). Apart from electrical coupling, transplanted cells must achieve functional integration in order to avoid the appearance of arrhythmias. For this, cells must be electromechanically similar to the endogenous adult myocardium (Pijnappels *et al.*, 2010), which supports the transplantation of differentiated CMs instead of stem cells.

Finally, we were able to confirm that the long-term engraftment of hiPSC-CMs resulted in the repair of the damaged cardiac tissue, which is the final objective of this strategy. The enhanced cardiac function observed could result from a dual action of particles and cells, since MPs alone were able to improve cardiac output and stroke volume (data not shown). In line with this, no significant differences were found between the MPs and hiPSC-CM-MPs groups in infarct size and left ventricle wall thickness. These results could be due to the mechanical reinforcement that particles provide to the ventricle wall, which increases wall thickness, prevents infarct expansion and therefore, enhances the function of the host myocardium. Besides that, cardiac repair is mainly attributed to the delivered cells. Interestingly, the significant prevention in the increase of ESV and EDV after 2 months, reflect that the combinatorial treatment avoided the enlargement of the left ventricle to compensate for the loss of function. The low engraftment of transplanted hiPSC-CMs evidences that cells stimulate cardiac repair by the paracrine secretion of growth factors/cytokines. It has been previously described that hiPSC-CMs secrete anti-apoptotic, pro-angiogenic and cell migration related factors (Tachibana *et al.*, 2017). These results are in agreement with recent experiments by Tachibana et al. (Tachibana *et al.*, 2017) and Zhu et al. (Zhu *et al.*, 2018) attributing to the paracrine effect the functional improvements observed after

transplantation of cardiac myocytes or cardiovascular progenitors. Moreover, the lack of evident sarcomeric striations 2 months after transplantation further points to the paracrine capacity over contractile support as the driver of the functional benefit.

In summary, the findings of the present study confirm that biomimetic particles represent an excellent platform to improve long-term cell engraftment, due to their ability to create a favourable microenvironment that retains cells at the injection site and supports cell functions. Future studies should focus on the mechanisms responsible for the therapeutic response observed, such as characterization of the paracrine secretion of hiPSC-CMs, as well as its impact on the endogenous tissue. Furthermore, specific molecules could be incorporated into MPs to direct transplanted cells function, as shown in other studies (Mahoney and Saltzman, 2001). It should also be considered that in this study, cells of human origin were injected in a mouse MI model. The use of more representative models of human physiology (pig or non-human primate) could help to elucidate the potential of hiPSC-CMs combined with MPs to directly remuscularize infarcted tissue. Finally, this platform could be implemented not only in the field of cardiac repair, but also in other areas of regenerative medicine.

Authorship Contributions

Participated in research design: L.S., E.G., M.M., F.P., B.P., A. R., M.B.P.

Conducted experiments: L.S., E.G., M.M., B.P., G.A., O.I.G.

Performed data analysis: L.S., E.G., M.M., B.P and G.A.

Wrote or contributing in the writing of the manuscript: L.S., E.G., M.M., B.P., F.P. and M.B.P.

References

Ahrens CC, Dong Z, and Li W (2017) Engineering cell aggregates through incorporated polymeric microparticles. *Acta Biomater* **62**:64–81.

Atluri P, Miller JS, Emery RJ, Hung G, Trubelja A, Cohen JE, Lloyd K, Han J, Gaffey AC, Macarthur JW, Chen CS, and Woo YJ (2014) Tissue-engineered, hydrogel-based endothelial progenitor cell therapy robustly revascularizes ischemic myocardium and preserves ventricular function. *J Thorac Cardiovasc Surg* **148**:1090–1098.

Bahit MC, Kochar A, and Granger CB (2018) Post-myocardial infarction heart failure. *JACC Hear Fail* **6**:179–186.

Batalov I, and Feinberg AW (2015) Differentiation of cardiomyocytes from human pluripotent stem cells using monolayer culture. *Biomark Insights* **10**:71–6.

Benavides-Vallve C, Corbacho D, Iglesias-Garcia O, Pelacho B, Albiasu E, Castaño S, Muñoz-Barrutia A, Prosper F, and Ortiz-de-Solorzano C (2012) New strategies for echocardiographic evaluation of left ventricular function in a mouse model of long-term myocardial infarction. *PLoS One* **7**:e41691.

Boheler KR, Czyz J, Tweedie D, Yang H-T, Anisimov S V, and Wobus AM (2002) Differentiation of pluripotent embryonic stem cells into cardiomyocytes. *Circ Res* **91**:189–201.

Breckwoldt K, Letuffe-Brenière D, Mannhardt I, Schulze T, Ulmer B, Werner T, Benzin A, Klampe B, Reinsch MC, Laufer S, Shibamiya A, Prondzynski M, Mearini G, Schade D, Fuchs S, Neuber C, Krämer E, Saleem U, Schulze ML, Rodriguez ML, Eschenhagen T, and Hansen A (2017) Differentiation of cardiomyocytes and generation of human engineered heart tissue. *Nat Protoc* **12**:1177–1197.

Cahill TJ, Choudhury RP, and Riley PR (2017) Heart regeneration and repair after myocardial infarction: translational opportunities for novel therapeutics. *Nat Rev Drug Discov* **16**:699–

717.

Chow A, Stuckey DJ, Kidher E, Rocco M, Jabbour RJ, Mansfield CA, Darzi A, Harding SE, Stevens MM, and Athanasiou T (2017) Cardiomyocyte encapsulating bioactive hydrogels improve rat heart function post myocardial infarction. *Stem cell reports* **9**:1415–1422.

Delcroix GJ, Garbayo E, Sindji L, Thomas O, Vanpouille-Box C, Schiller PC, and Montero-Menei CN (2011) The therapeutic potential of human multipotent mesenchymal stromal cells combined with pharmacologically active microcarriers transplanted in hemi-parkinsonian rats. *Biomaterials* **32**:1560–1573.

Díaz-Herráez P, Garbayo E, Simón-Yarza T, Formiga FR, Prosper F, and Blanco-Prieto MJ (2013) Adipose-derived stem cells combined with neuregulin-1 delivery systems for heart tissue engineering. *Eur J Pharm Biopharm* **85**:143–150.

Díaz-Herráez P, Saludas L, Pascual-Gil S, Simón-Yarza T, Abizanda G, Prósper F, Garbayo E, and Blanco-Prieto MJ (2017) Transplantation of adipose-derived stem cells combined with neuregulin-microparticles promotes efficient cardiac repair in a rat myocardial infarction model. *J Control Release* **249**:23–31.

Formiga FR, Garbayo E, Díaz-Herráez P, Abizanda G, Simón-Yarza T, Tamayo E, Prósper F, and Blanco-Prieto MJ (2013) Biodegradation and heart retention of polymeric microparticles in a rat model of myocardial ischemia. *Eur J Pharm Biopharm* **85**:665–72.

Garbayo E, Gavira J, Garcia de Yebenes M, Pelacho B, Abizanda G, Lana H, Blanco-Prieto M, and Prosper F (2016) Catheter-based intramyocardial injection of FGF1 or NRG1-loaded MPs improves cardiac function in a preclinical model of ischemia-reperfusion. *Sci Rep* **6**:25932.

Garbayo E, Raval AP, Curtis KM, Della-Morte D, Gomez LA, D'Ippolito G, Reiner T, Perez-Stable C, Howard GA, Perez-Pinzon MA, Montero-Menei CN, and Schiller PC (2011) Neuroprotective properties of marrow-isolated adult multilineage-inducible cells in rat

hippocampus following global cerebral ischemia are enhanced when complexed to biomimetic microcarriers. *J Neurochem* **119**:972–88.

Gepstein L (2002) Derivation and potential applications of human embryonic stem cells. *Circ Res* **91**:866–76.

Hodgkinson CP, Bareja A, Gomez JA, and Dzau VJ (2016) Emerging concepts in paracrine mechanisms in regenerative cardiovascular medicine and biology. *Circ Res* **118**:95–107.

Hou D, Youssef EA-S, Brinton TJ, Zhang P, Rogers P, Price ET, Yeung AC, Johnstone BH, Yock PG, and March KL (2005) Radiolabeled cell distribution after intramyocardial, intracoronary, and interstitial retrograde coronary venous delivery: implications for current clinical trials. *Circulation* **112**:I150-6.

Iglesias-García O, Baumgartner S, Macrí-Pellizzeri L, Rodriguez-Madoz JR, Abizanda G, Guruceaga E, Albiasu E, Corbacho D, Benavides-Vallve C, Soriano-Navarro M, González-Granero S, Gavira JJ, Krausgrill B, Rodriguez-Mañero M, García-Verdugo JM, Ortiz-de-Solorzano C, Halbach M, Hescheler J, Pelacho B, and Prósper F (2015) Neuregulin-1β induces mature ventricular cardiac differentiation from induced pluripotent stem cells contributing to cardiac tissue repair. *Stem Cells Dev* **24**:484–96.

Lalit PA, Hei DJ, Raval AN, and Kamp TJ (2014) Induced pluripotent stem cells for post-myocardial infarction repair: remarkable opportunities and challenges. *Circ Res* **114**:1328–45.

Leong W, and Wang D-A (2015) Cell-laden polymeric microspheres for biomedical applications. *Trends Biotechnol* **33**:653–666.

Lian X, Zhang J, Azarin SM, Zhu K, Hazeltine LB, Bao X, Hsiao C, Kamp TJ, and Palecek SP (2013) Directed cardiomyocyte differentiation from human pluripotent stem cells by modulating Wnt/β-catenin signaling under fully defined conditions. *Nat Protoc* **8**:162–175.

Lin YD, Yeh ML, Yang YJ, Tsai DC, Chu TY, Shih YY, Chang MY, Liu YW, Tang ACL, Chen TY, Luo CY, Chang KC, Chen JH, Wu HL, Hung TK, and Hsieh PCH (2010) Intramyocardial peptide nanofiber injection improves postinfarction ventricular remodeling and efficacy of bone marrow cell therapy in pigs. *Circulation* **122**:S132-41.

Liu Y-W, Chen B, Yang X, Fugate JA, Kalucki FA, Futakuchi-Tsuchida A, Couture L, Vogel KW, Astley CA, Baldessari A, Ogle J, Don CW, Steinberg ZL, Seslar SP, Tuck SA, Tsuchida H, Naumova A V, Dupras SK, Lyu MS, Lee J, Hailey DW, Reinecke H, Pabon L, Fryer BH, MacLellan WR, Thies RS, and Murry CE (2018) Human embryonic stem cell–derived cardiomyocytes restore function in infarcted hearts of non-human primates. *Nat Biotechnol* **36**:597–605.

Mahoney MJ, and Saltzman WM (2001) Transplantation of brain cells assembled around a programmable synthetic microenvironment. *Nat Biotechnol* **19**:934–9.

Nigro P, Bassetti B, Cavallotti L, Catto V, Carbucicchio C, and Pompilio G (2018) Cell therapy for heart disease after 15 years: Unmet expectations. *Pharmacol Res* **127**:77–91.

Nussbaum J, Minami E, Laflamme MA, Virag JAI, Ware CB, Masino A, Muskheli V, Pabon L, Reinecke H, and Murry CE (2007) Transplantation of undifferentiated murine embryonic stem cells in the heart: teratoma formation and immune response. *FASEB J* **21**:1345–1357.

Pascual-Gil S, Simón-Yarza T, Garbayo E, Prosper F, and Blanco-Prieto MJ (2015) Tracking the in vivo release of bioactive NRG from PLGA and PEG-PLGA microparticles in infarcted hearts. *J Control Release* **220**:388–396.

Pijnappels DA, Gregoire S, and Wu SM (2010) The integrative aspects of cardiac physiology and their implications for cell-based therapy. *Ann N Y Acad Sci* **1188**:7–14.

Reed GW, Rossi JE, and Cannon CP (2017) Acute myocardial infarction. *Lancet* **389**:197–210.

Roell W, Lewalter T, Sasse P, Tallini YN, Choi B-R, Breitbach M, Doran R, Becher UM, Hwang S-M, Bostani T, von Maltzahn J, Hofmann A, Reining S, Eiberger B, Gabris B,

Pfeifer A, Welz A, Willecke K, Salama G, Schrickel JW, Kotlikoff MI, and Fleischmann BK (2007) Engraftment of connexin 43-expressing cells prevents post-infarct arrhythmia. *Nature* **450**:819–824.

Saludas L, Pascual-Gil S, Prósper F, Garbayo E, and Blanco-Prieto M (2017) Hydrogel based approaches for cardiac tissue engineering. *Int J Pharm* **523**:454–475.

Saludas L, Pascual-Gil S, Roli F, Garbayo E, and Blanco-Prieto MJ (2018) Heart tissue repair and cardioprotection using drug delivery systems. *Maturitas* **110**:1–9.

Suarez SL, Muñoz A, Mitchell AC, Braden RL, Luo C, Cochran JR, Almutairi A, and Christman KL (2016) Degradable acetalated dextran microparticles for tunable release of an engineered hepatocyte growth factor fragment. *ACS Biomater Sci Eng* **2**:197–204.

Tachibana A, Santoso MR, Mahmoudi M, Shukla P, Wang L, Bennett M, Goldstone AB, Wang M, Fukushi M, Ebert AD, Woo YJ, Rulifson E, and Yang PC (2017) Paracrine effects of the pluripotent stem cell-derived cardiac myocytes salvage the injured myocardium. *Circ Res* **121**:e22–e36.

Takahashi K, and Yamanaka S (2006) Induction of pluripotent stem cells from mouse embryonic and adult fibroblast cultures by defined factors. *Cell* **126**:663–676.

Telukuntla KS, Suncion VY, Schulman IH, and Hare JM (2013) The advancing field of cell-based therapy: insights and lessons from clinical trials. *J Am Heart Assoc* **2**:e000338.

Terrovitis J V, Smith RR, and Marbán E (2010) Assessment and optimization of cell engraftment after transplantation into the heart. *Circ Res* **106**:479–94.

Tonsho M, Michel S, Ahmed Z, Alessandrini A, and Madsen JC (2014) Heart transplantation: challenges facing the field. *Cold Spring Harb Perspect Med* **4**.

Wang H, Xi Y, Zheng Y, Wang X, and Cooney AJ (2016) Generation of electrophysiologically functional cardiomyocytes from mouse induced pluripotent stem cells. *Stem Cell Res* **16**:522–530.

Wang X, Chun YW, Zhong L, Chiusa M, Balikov DA, Frist AY, Lim CC, Maltais S, Bellan L, Hong CC, and Sung H-J (2015) A temperature-sensitive, self-adhesive hydrogel to deliver iPSC-derived cardiomyocytes for heart repair. *Int J Cardiol* **190**:177–80.

Yu H, Lu K, Zhu J, and Wang J (2017) Stem cell therapy for ischemic heart diseases. *Br Med Bull* **121**:135–154.

Zhu K, Wu Q, Ni C, Zhang P, Zhong Z, Wu Y, Wang Y, Xu Y, Kong M, Cheng H, Tao Z, Yang Q, Liang H, Jiang Y, Li Q, Zhao J, Huang J, Zhang F, Chen Q, Li Y, Chen J, Zhu W, Yu H, Zhang J, Yang H-T, Hu X, and Wang J (2018) Lack of remuscularization following transplantation of human embryonic stem cell-derived cardiovascular progenitor cells in infarcted nonhuman primates. *Circ Res* **122**:958–969.

Footnotes

This work was supported by the Spanish Ministry of Economy and Competitiveness [SAF2013-42528-R, SAF2017-83734-R and Cardiomesh], funds from the ISCIII and FEDER [Tercel RD16/0011/0005, PI16/00129, CPII15/00017 and ERANET II-Nanoreheart], "Asociación de Amigos de la Universidad de Navarra" and "la Caixa" Banking Foundation.

Figure Legends

Figure 1. Cardiac differentiation of hiPSCs. A) Diagram of small molecule-based CM differentiation and metabolic selection. B) Representative FACS staining for cTnT, showing a purity of >90% of hiPSC-CMs. C) Gene expression profile of hiPSC-CMs, demonstrating proper downregulation of pluripotency genes (NANOG, POU5F1 and SOX2) and upregulation of cardiac transcription factors (NKX2-5, GATA4, MEF2C) and contractile proteins (MYH6, MYH7); co-expression of genes for CM subtypes is detected, namely ventricular (MYL2), atrial (MYL7) and pacemaker (HCN4). D) Immunofluorescence for α-sarcomeric actinin, confirming the high purity of cultures (i), with cells displaying evident sarcomeric striations (ii). Data represented as mean ± SD. Scale bars: Di: 25 μm; Dii: 10 μm.

Figure 2. Adhesion of hiPSC-CMs to biomimetic MPs and *in vitro* cell viability. A) Bright field images of the complexes formed by 150,000 hiPSC-CMs and 0.150 mg of MPs covered with different mixtures of biomimetic molecules after 1.5 hours of incubation. MPs coated with 30 μg/ml of collagen type I and 100 μg/ml of PDL showed the largest adhesion of hiPSC-CMs and were selected for further studies. B) Representative confocal images of hiPSCs cultured alone or in combination with biomimetic MPs for 24 hours. Calcein AM (green) stains for live cells and ethidium homodimer-1 (red) for dead cells. Scale bar: 50 μm.

Figure 3. Effects of hiPSC-CM-MPs on cardiac function. LVEF (A), FAC (B), ESV (C) and EDV (D) measured by echocardiography at 2 days and at 2 months post-treatment in animals injected with MPs alone or with hiPSC-CMs adhered to biomimetic MPs (hiPSC-CM-MPs). Results show that combinatorial treatment of MPs and hiPSC-CMs improves cardiac function after 2 months compared to MPs. Data are expressed as mean ± SEM (t test for independent samples, * $p < 0.05$, ** $p < 0.01$).

Figure 4. Effects of hiPSC-CM-MPs on ventricle remodeling. Representative images and quantification of left ventricle (LV) wall thickness (A) and infarct size (B) as measured by Sirius Red staining after 2 months of treatment administration. Both treatment groups presented similar

wall thickness of the left ventricle, whereas administration of hiPSC-CM-MPs showed a tendency to reduce infarct size. Data are expressed as mean ± SEM. Scale bars: A) 1 mm, B) 100 μm.

Figure 5. Fate of hiPSC-CMs after transplantation in the cardiac tissue. A) Analysis of cell engraftment and survival at 1 week and 2 months post-administration into the hearts of infarcted mice. Representative areas of infarcted myocardium showing hiPSC-CMs (h-MITO, green) engrafted in the tissue at both time points (area delimited by a discontinuous line). B) Expression of dystrophin (DYS, red) was observed in transplanted hiPSC-CMs after 2 months (arrow) suggesting that these cells maintained a cardiac phenotype. C) Engrafted hiPSC-CMs expressed the gap junction protein connexin-43 (CX-43, red) at the interface between cardiomyocytes suggesting electrical coupling 2 months post-administration (arrows). Scale bars: 50 μm.

JPET Fast Forward. Published on February 6, 2019 as DOI: 10.1124/jpet.118.256065
This article has not been copyedited and formatted. The final version may differ from this version.

Figures

Figure 1.

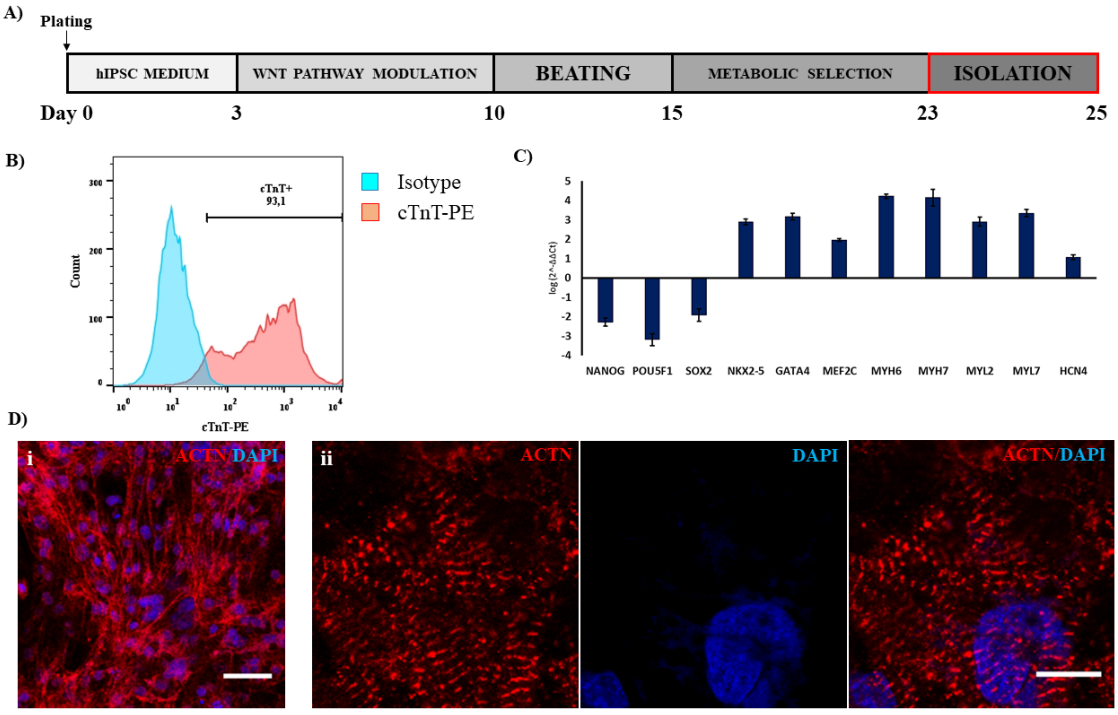

JPET Fast Forward. Published on February 6, 2019 as DOI: 10.1124/jpet.118.256065
This article has not been copyedited and formatted. The final version may differ from this version.

Figure 2.

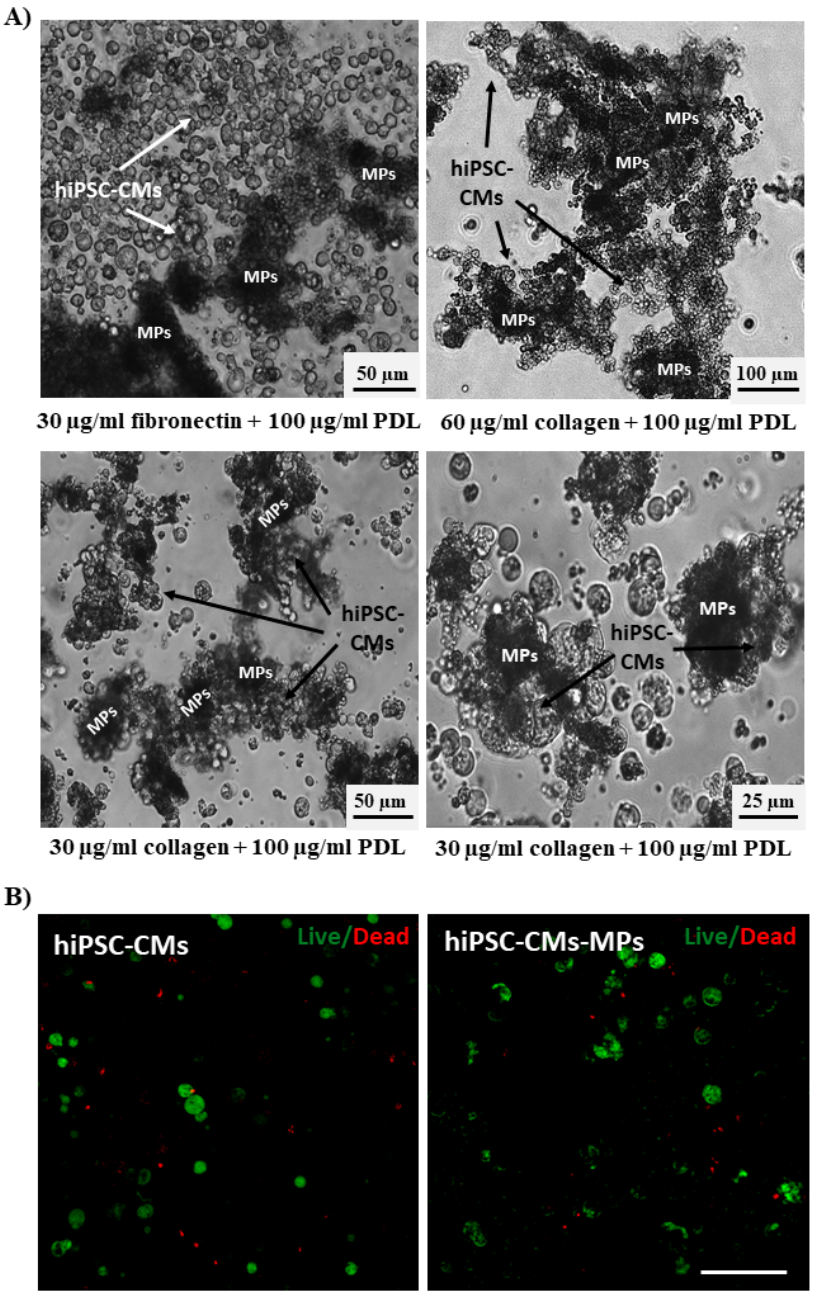

JPET Fast Forward. Published on February 6, 2019 as DOI: 10.1124/jpet.118.256065
This article has not been copyedited and formatted. The final version may differ from this version.

Figure 3.

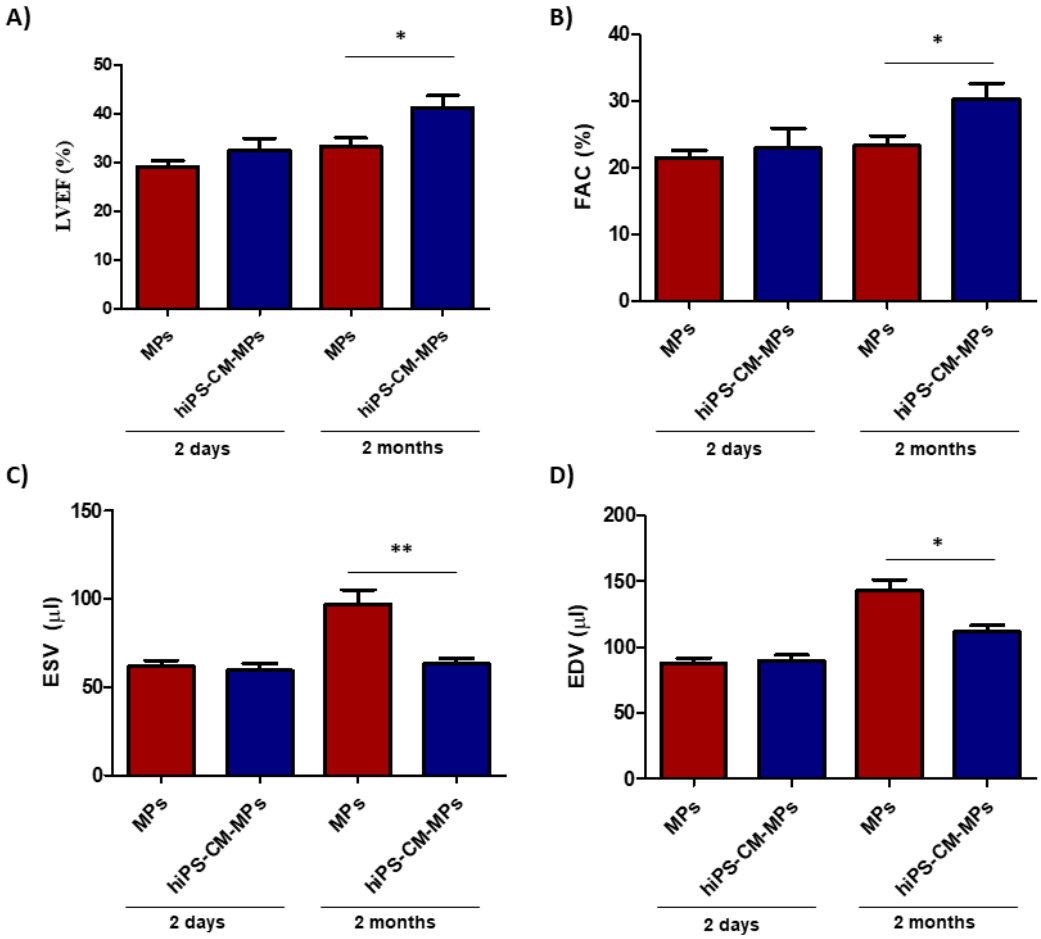

JPET Fast Forward. Published on February 6, 2019 as DOI: 10.1124/jpet.118.256065
This article has not been copyedited and formatted. The final version may differ from this version.

Figure 4.

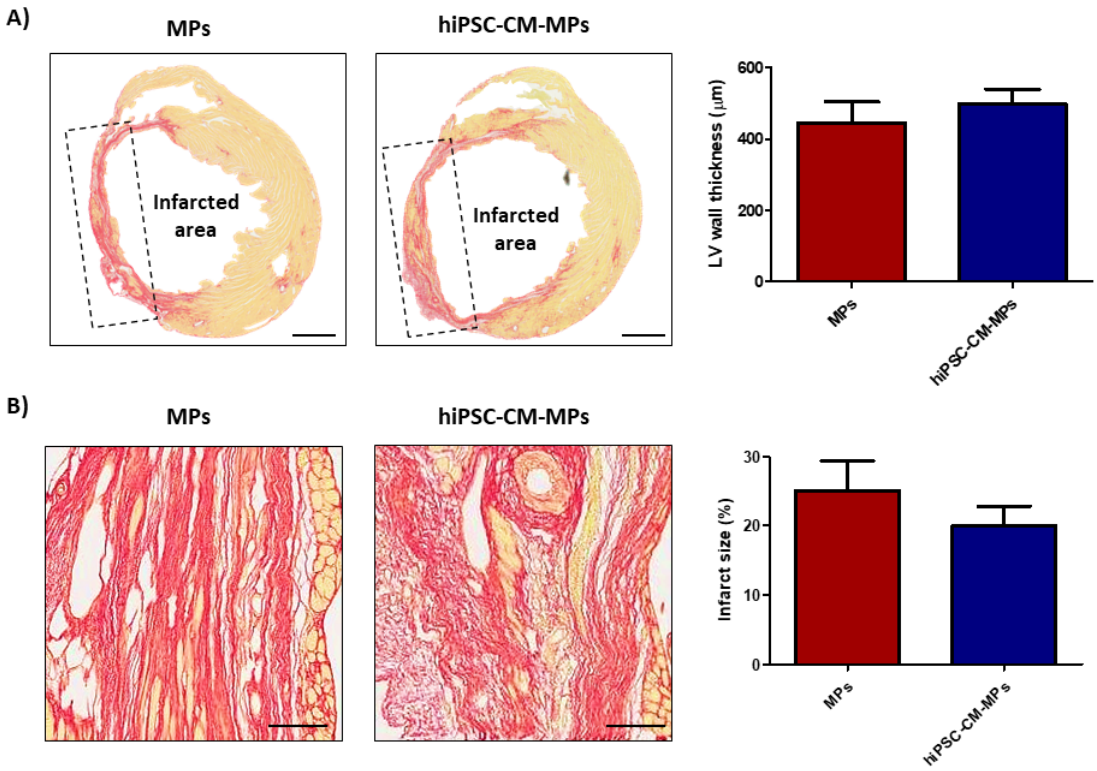

JPET Fast Forward. Published on February 6, 2019 as DOI: 10.1124/jpet.118.256065
This article has not been copyedited and formatted. The final version may differ from this version.

Figure 5.

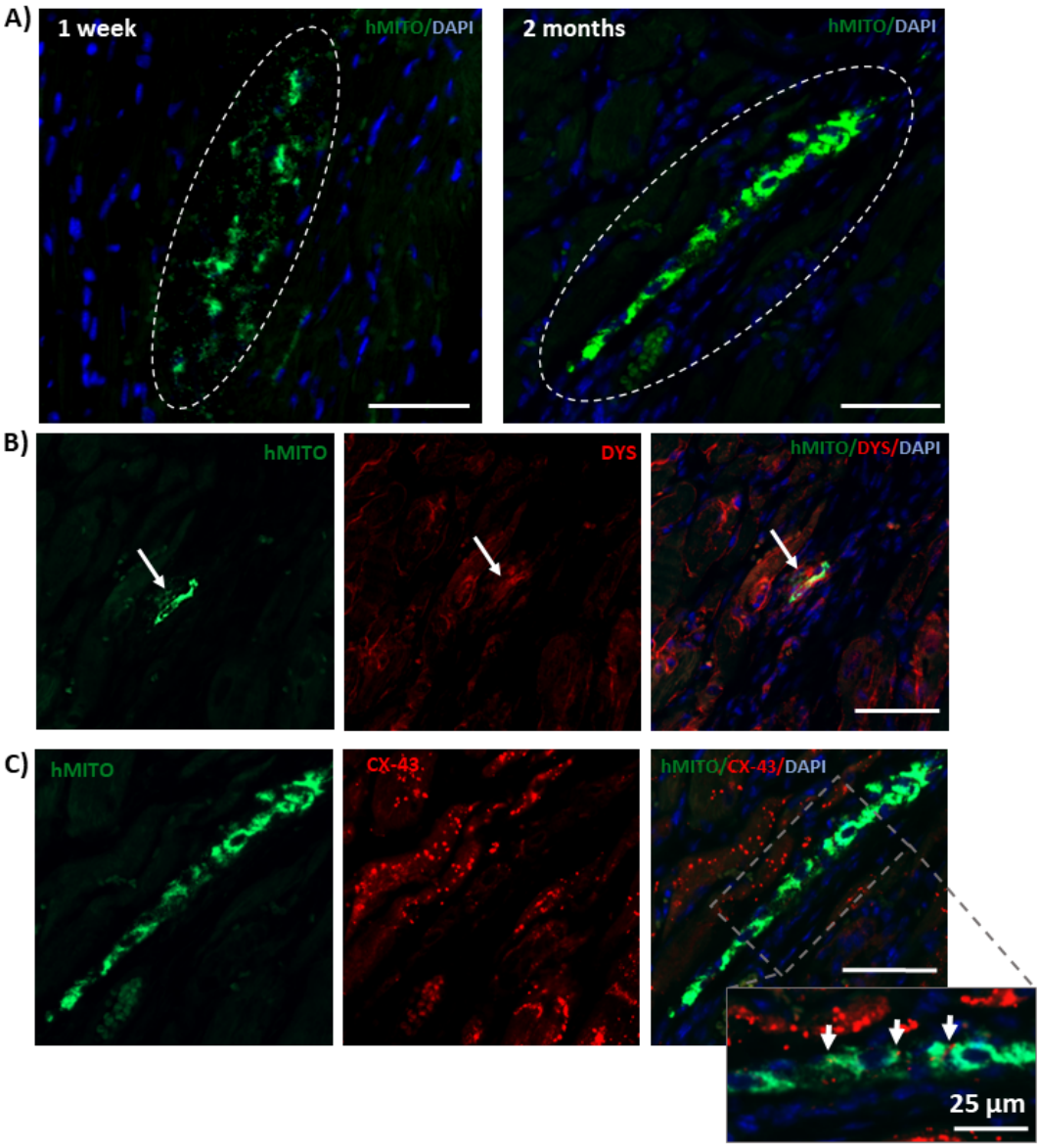

Supplemental Data

Long-term engraftment of human cardiomyocytes combined with biodegradable microparticles induces heart repair

Laura Saludas*, Elisa Garbayo*, Manuel Mazo, Beatriz Pelacho, Gloria Abizanda, Olalla Iglesias-García, Ángel Raya, Felipe Prósper, María J. Blanco-Prieto

* Both authors contributed equally to this work

The Journal of Pharmacology and Experimental Therapeutics

Table 1. Primers used in RT-PCR analysis of hiPSC-CMs.

Gene	Forward Primer	Reverse Primer
GAPDH	TGGTATCGTGGAAGGACTCATGA	ATGCCAGTGAGCTTCCCGTTCAG
NANOG	GATTTGTGGGCCTGAAGAAA	CAGATCCATGGAGGAAGGAA
POU5F1	GGCTCGAGAAGGATGTGGT	GTTGTGCATAGTCGCTGCTT
SOX2	AACGGCAGCTACAGCATGA	ATGTAGGTCTGCGAGCTGGT
NKX2-5	ACCCAGCCAAGGACCCTA	TTGTCCGCCTCTGTCTTCTC
GATA4	GCGAGCCTGTGTGCAATG	CTGGTTTGGATCCCCTCTTT
MEF2C	CCACCAGGCAGCAAGAATAC	TGGGGTAGCCAATGACTGAG
MYH6	GGAGGGAGGCAAGGTCAT	GGTTCTGCTGCAACACCTG
MYH7	ATGCATTCATCTCCCAAGGA	GAAGCCCAGCACATCAAAAG
MYL2	CAACGTGTTCTCCATGTTCG	GTCAATGAAGCCATCCCTGT
MYL7	CCCATCAACTTCACCGTCTT	AGGCACTCAGGATGGCTTC
HCN4	CGGCCGGATTTTGGATTAT	AATCAGGTTTCCCACCATCA